

What is the best proton energy for accelerator-based BNCT using the ${}^7\text{Li}(p,n){}^7\text{Be}$ reaction?

D. A. Allen and T. D. Beynon

School of Physics and Astronomy, University of Birmingham, Edgbaston, Birmingham, B15 2TT, United Kingdom

(Received 29 September 1999; accepted for publication 15 February 2000)

With a growing interest in the use of accelerator-based epithermal neutron sources for BNCT programs, in particular those based upon the ${}^7\text{Li}(p,n){}^7\text{Be}$ reaction, there is a need to address the question of “what is the best proton energy to use?” This paper considers this question by using radiation transport calculations to investigate a range of proton energies from 2.15 to 3.5 MeV and a range of moderator sizes. This study has moved away completely from the use of empty therapy beam parameters and instead defines the beam quality and optimizes the moderator design using widely accepted in-phantom treatment planning figures of merit. It is concluded that up to a proton energy of about 2.8 MeV there is no observed variation in the achievable therapy beam quality, but a price is paid in terms of treatment time for not choosing the upper limit of this range. For higher proton energies, the beam quality falls, but with no improvement in treatment time for optimum configurations. © 2000 American Association of Physicists in Medicine. [S0094-2405(00)00605-2]

Key words: BNCT, MCNP, accelerator, epithermal neutrons, radiotherapy

I. INTRODUCTION

Accelerator-based neutron sources are becoming increasingly popular for research programs into boron neutron capture therapy (BNCT). The advantages of such sources are listed elsewhere,¹ the main ones being low cost and the possibility of siting small accelerator-based sources actually within a hospital environment.

Of all the possible neutron-producing reactions, the most popular choice appears to be ${}^7\text{Li}(p,n){}^7\text{Be}$. This is due to its high yield at low proton energies and its endothermic nature ($Q = -1.644$ MeV), which means that the neutrons produced have a relatively low mean energy. However, due to the high proton current requirements, high power targets are required and appropriate cooling systems must be developed in order to exploit this reaction for clinical BNCT.

Given the critical significance that the neutron source has in a BNCT system, it is most important that we consider not only which is the best target to use, but also what is the best proton energy to use. Other authors have proffered answers to this question based on consideration of empty neutron therapy beam parameters, using concepts such as “useful” neutron fluence rate, mean neutron energy and neutron dose rate per unit “useful” epithermal neutron fluence.^{2–4} However, empty beam parameters are of limited value in describing an accelerator-based BNCT neutron beam, since the close proximity of the patient or phantom to the moderator/filter assembly results in a very high degree of neutronic coupling. This means that any derived empty beam fluence rate, dose rate or spectrum is immediately altered once a patient or phantom is introduced to the therapy position. This paper attempts to answer the question of what is the best proton energy to use with a thick lithium target, using arguments based exclusively on the results of coupled source,

moderator and phantom computer simulations. In this way the problems associated with empty beam parameters are circumvented by going straight to a consideration of in-phantom figures of merit. A paper by Bleuel *et al.*⁵ on more general aspects of BNCT moderator design also considers the question of proton energy, but only over a more limited range using two-stage noncoupled moderator and phantom simulations.

The cross section for the ${}^7\text{Li}(p,n){}^7\text{Be}$ reaction has a proton threshold energy of 1.88 MeV and shows a resonance peak at 2.25 MeV. This study has investigated the following proton energies for suitability: 2.15, 2.25, 2.4, 2.8, 3.1 and 3.5 MeV, representing energies below, at, just above and well above the resonance. Higher proton energies have not been investigated because the higher mean energy of the neutrons produced counteracts one of the chief physical advantages of using an accelerator-based source. Near-threshold concepts have been considered elsewhere.⁶

II. THE COMPUTER MODEL

At each proton energy considered, the neutron yield from a thick natural lithium target was calculated as a function of angle and energy using the method described in Ref. 1 and the double-differential cross-section data of Liskien and Paulsen.⁷ A total of 18 angle bins were used to cover the full range, and the width of each energy bin was 10 keV. The total yields were taken from the experimental data of Campbell and Scott.⁸

The calculated neutron yields were then used as the source terms in a series of neutron and coupled neutron-photon Monte Carlo simulations using the general purpose code MCNP.⁹ This code was used to simulate the transport of neutrons and neutron-generated photons throughout the tar-

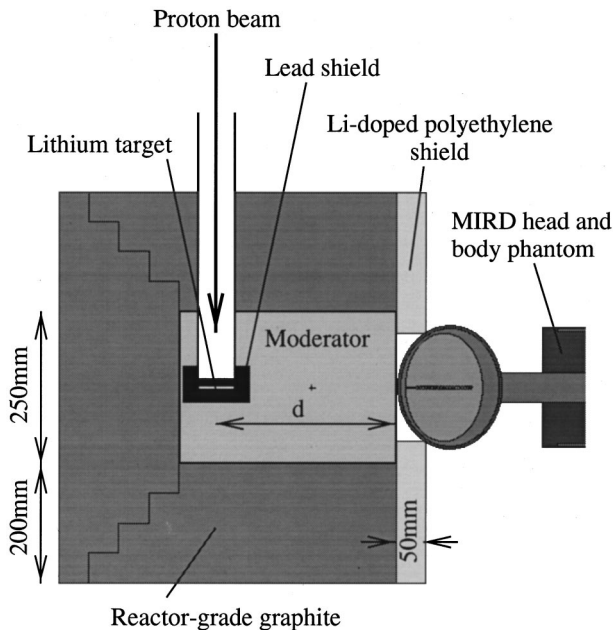


FIG. 1. A sectional view through the moderator and phantom axis of the geometry used for the Monte Carlo simulations.

get, moderator, reflector, shield and phantom, using the geometry depicted in Fig. 1. The proton beam was assumed to be uniform over a diameter of 50 mm. A previous study has shown that the diameter of the source term has little effect upon the quality of the orthogonally extracted neutron therapy beam for source diameters up to about 75 mm.¹⁰

The moderator material chosen consists of aluminum (43.2%), fluorine (55.9%) and natural lithium (0.9%). This is a popular choice of BNCT moderator/filter material, based on an original idea proposed in Ref. 11, which is subsequently being used by several existing and proposed BNCT facilities. The main advantage of moderators with this composition is that neutrons within the energy range of 20 to 400 keV are preferentially scattered to lower energies, where the cross section is much lower, by the complementary resonances found in aluminum and fluorine. After moderation, the epithermal neutron beam in our design is extracted in an orthogonal direction to the incoming proton beam as described in Ref. 10, and is delimited using a 50 mm thick natural lithium-doped polyethylene shield with a 180 mm diameter aperture. It is recognized that the choice of moderating material may affect the conclusions reached in this study regarding the optimum moderator dimension for each proton energy.

Various thicknesses of moderating material were used in this study and the individual dose components were calculated as a function of depth in the phantom using track length cell flux tallies. The tally cells were spheres of diameters ranging from 5 mm, at the center of the brain where the flux is low, to 2.5 mm near the surface. This change in tally cell size, together with a judicious use of variance reduction methods, enabled relatively rapid calculations whilst maintaining acceptable statistical uncertainties for all of the tallies. The moderator thickness is denoted by d in Fig. 1 and is

TABLE I. The calculated dose components together with the relative biological effectiveness and compound biological effectiveness factors used for this study.

Dose component	RBE/CBE
Proton recoil ${}^1\text{H}(n,n'){}^1\text{H}$	RBE=3.2 ^a
Nitrogen ${}^{14}\text{N}(n,p){}^{14}\text{C}$ (neutron)	RBE=3.2 ^a
Photons	RBE=1.0
${}^{10}\text{B}(n,\alpha){}^7\text{Li}$ to normal tissue	CBE=1.3 ^b
${}^{10}\text{B}(n,\alpha){}^7\text{Li}$ to tumor tissue	CBE=3.8 ^b

^aReference 14.

^bReference 15.

the distance between the axis of the incoming proton beam and the exit surface of the neutron therapy beam.

The phantom used was a standard MIRD design¹² modified by the inclusion of a 5 mm scalp as described by Liu *et al.*¹³ In addition to the head model often used, the whole body MIRD phantom has been included, since reflected neutrons and photons from the upper torso can make significant contributions to the head phantom dose rates—up to 10% at 110 mm depth in this study. The axis of the phantom was aligned with that of the moderator and the top of the head was placed against the moderator exit surface with a 2 mm clearance. All of the in-phantom dose-depth distributions calculated were as a function of depth into the brain, not the whole phantom. Thus the center of the brain is at a depth along the phantom axis of 65 mm, or 78 mm into the phantom from the top; the combined thickness of scalp and skull being 13 mm in this phantom at this position. A ${}^{10}\text{B}$ concentration of $15\mu\text{g/g}$ was included throughout the whole phantom.

Table I lists the dose components that were calculated for each tally cell and the RBE/CBE (relative biological effectiveness/compound biological effectiveness) factors which were applied to calculate the biologically weighted doses. The CBE figures used assume that BPA (boronophenylalanine) is the boron delivery agent.

The RBE for neutron dose components will be beam dependent and is, in any case, subject to considerable uncertainty. In order to gain some insight into the effect that this uncertainty may have upon beam design studies, we have repeated the calculations using a neutron RBE of 4.5 for both neutron components, the other RBE/CBE factors being kept the same.

III. TREATMENT PLANNING FIGURE OF MERIT

This study uses the definitions in Ref. 16 for the in-phantom treatment planning figures of merit in order to determine the quality of each particular BNCT therapy beam. At any point within a phantom the *therapeutic ratio* (TR) is defined to be the ratio of the total biologically weighted dose to tumor at that point to the maximum biologically weighted dose to healthy tissue anywhere in the brain. In most cases the maximum dose to healthy tissue occurs at the surface of the brain where the neutron beam enters, but it may also occur at up to a few centimeters depth.

Figure 2 shows a typical set of biologically weighted in-phantom healthy tissue dose-depth curves for the dose com-

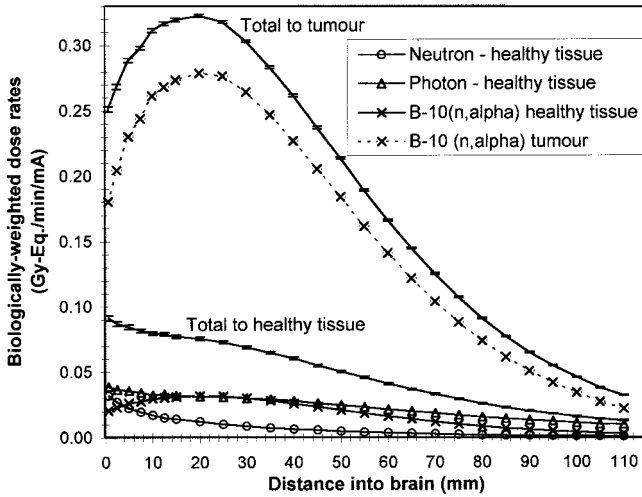


FIG. 2. Biologically weighted in-phantom dose distributions in healthy tissue using a 220 mm moderator with a 2.4 MeV proton beam source.

ponents considered. Also shown are the total biologically weighted doses to healthy tissue and to tumor. These curves have been calculated for the case of a 2.4 MeV proton beam on target and for a 220 mm moderator. The two neutron components have been combined, since they are weighted with the same RBE. The maximum dose to healthy tissue for this case is found at the surface of the brain and is 0.092 Gy-Eq per minute per mA of proton beam current. It is the maximum dose to healthy tissue which determines the notional *treatment time* for each beam configuration studied. In calculating the treatment time a maximum dose to healthy tissue of 12.6 Gy-Eq has been assumed, in accordance with the current Brookhaven BNCT clinical trials,¹⁷ and a beam current of 1 mA has been used. For a given proton energy, as the moderator is made smaller the fast neutron dose near the surface increases and eventually becomes the major dose component near the surface. For large moderators, the fast neutron dose becomes the least significant near-surface component. The contribution to the total photon dose in-phantom from a 320 mm moderator with a 2.8 MeV proton beam ranges from 22% near the brain surface to 10% at the thermal neutron peak.

Figure 3 shows the therapeutic ratio as a function of depth into brain for the case of a 2.4 MeV proton beam and a 220 mm moderator. These TR curves are of a very similar shape for all of the configurations studied, with a peak in value at around 15 mm to 20 mm into the brain. For the purposes of comparing beam quality this study uses the following criteria: (i) the TR at the center of the brain (65 mm), (ii) the maximum TR and (iii) the advantage depth (AD), which is defined in Ref. 16 as the depth into the brain at which the TR falls to 1.0. These quantities are indicated in Fig. 3.

IV. RESULTS AND DISCUSSION

Figures 4–9 present these calculated treatment planning figures of merit for all of the proton energies and moderator configurations studied, using both values for the neutron RBE. For simplicity, the AD for neutron RBE=4.5 is not

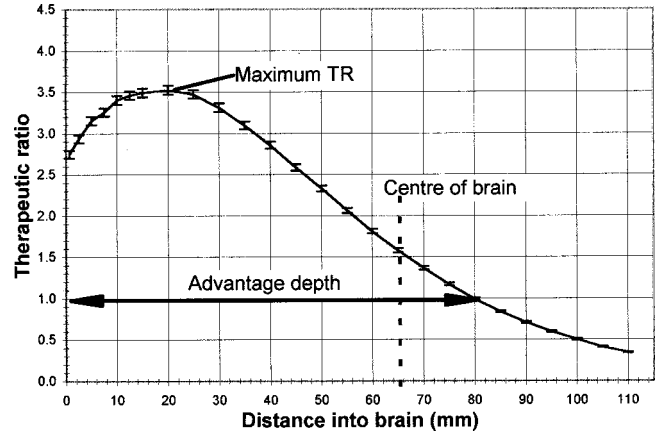


FIG. 3. The therapeutic ratio as a function of depth into brain for the case of the 2.4 MeV proton beam and 220 mm moderator.

plotted, since AD is not very sensitive to changes of this magnitude in the neutron RBE and the inclusion of these extra plots would add little to the following discussion. Figure 10 compares the treatment times for all of these configurations, using a neutron RBE of 3.2. There are a number of observations which can be made from these figures.

- (i) The treatment planning figures of merit do not change rapidly with changes in moderator depth. The choice of moderator depth is not, therefore, as critical a choice as would appear from the consideration of empty beam parameters.
- (ii) All of the curves for advantage depth and TR at the center of the brain show a broad peak over the range of moderator sizes considered. From the positions of these peaks the optimum moderator size range has

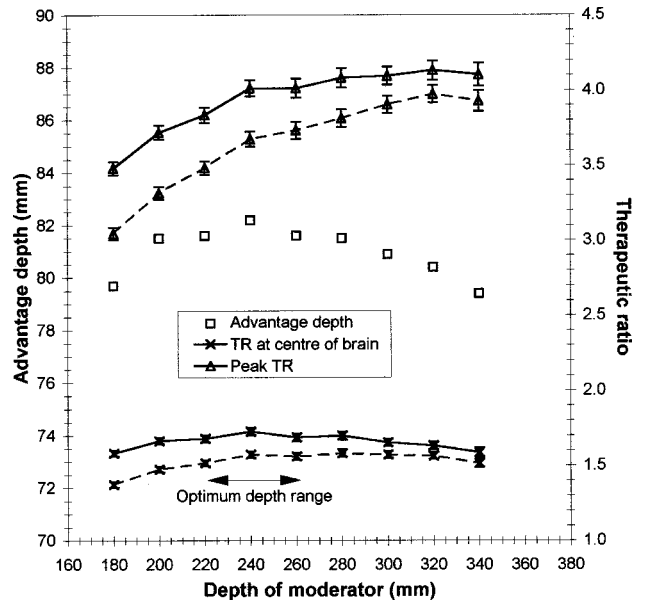


FIG. 4. The peak value of TR and TR at the center of the brain for various moderator sizes and a neutron source from 2.15 MeV protons. The range of optimum moderator size is indicated. Neutron RBE=3.2 (full lines) and 4.5 (dashed lines). The advantage depth for neutron RBE=3.2 is also plotted.

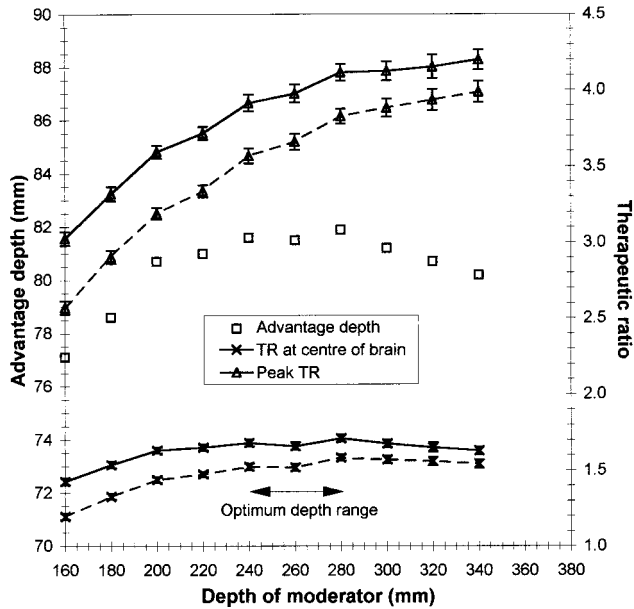


Fig. 5. The peak value of TR and TR at the center of the brain for various moderator sizes and a neutron source from 2.25 MeV protons. The range of optimum moderator size is indicated. Neutron RBE=3.2 (full lines) and 4.5 (dashed lines). The advantage depth for neutron RBE=3.2 is also plotted.

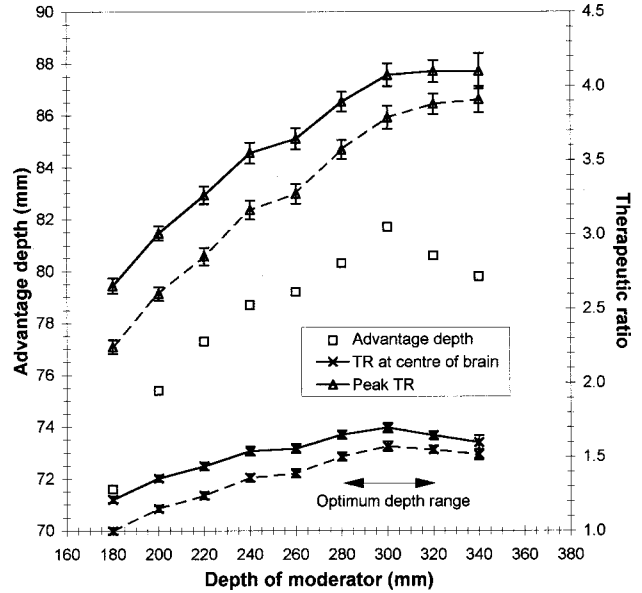


Fig. 7. The peak value of TR and TR at the center of the brain for various moderator sizes and a neutron source from 2.8 MeV protons. The range of optimum moderator size is indicated. Neutron RBE=3.2 (full lines) and 4.5 (dashed lines). The advantage depth for neutron RBE=3.2 is also plotted.

been identified for each proton energy, based on the assumption that maximizing the TR at the center of the brain and the AD are the main goals of optimization. These optimum ranges have been indicated on the figures for the case of neutron RBE=3.2.

- (iii) Of secondary significance is the peak value of the TR, which rises monotonically over the ranges considered, but tends to level off for large moderator sizes. For

this reason, the optimum moderator size for each proton energy has been chosen to be the upper limit of the ranges indicated in Figs. 4 to 9.

- (iv) The change of neutron RBE from 3.2 to 4.5 makes an obvious quantitative difference to the achievable treatment planning figures of merit, but very little qualitative difference to the shape of these curves. We might, however, decide to opt for a slightly larger moderator if we were using the figure of 4.5, although

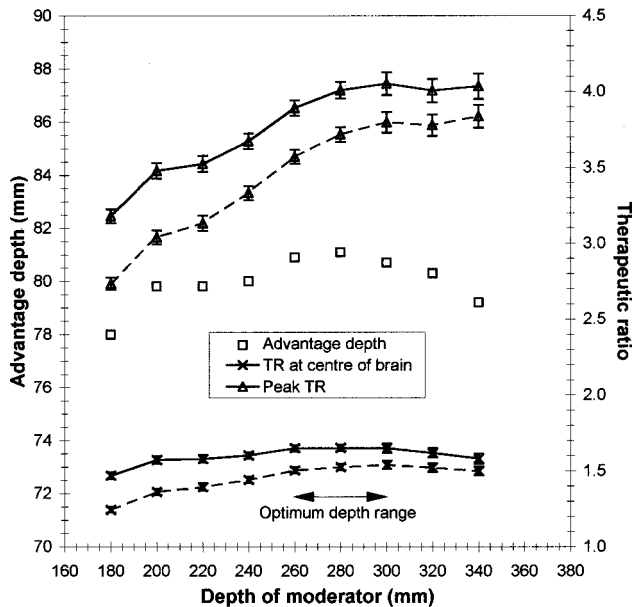


Fig. 6. The peak value of TR and TR at the center of the brain for various moderator sizes and a neutron source from 2.4 MeV protons. The range of optimum moderator size is indicated. Neutron RBE=3.2 (full lines) and 4.5 (dashed lines). The advantage depth for neutron RBE=3.2 is also plotted.

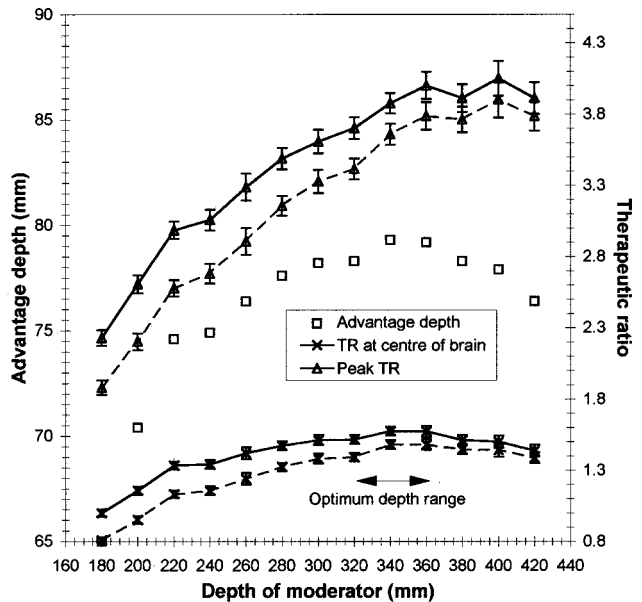


Fig. 8. The peak value of TR and TR at the center of the brain for various moderator sizes and a neutron source from 3.1 MeV protons. The range of optimum moderator size is indicated. Neutron RBE=3.2 (full lines) and 4.5 (dashed lines). The advantage depth for neutron RBE=3.2 is also plotted.

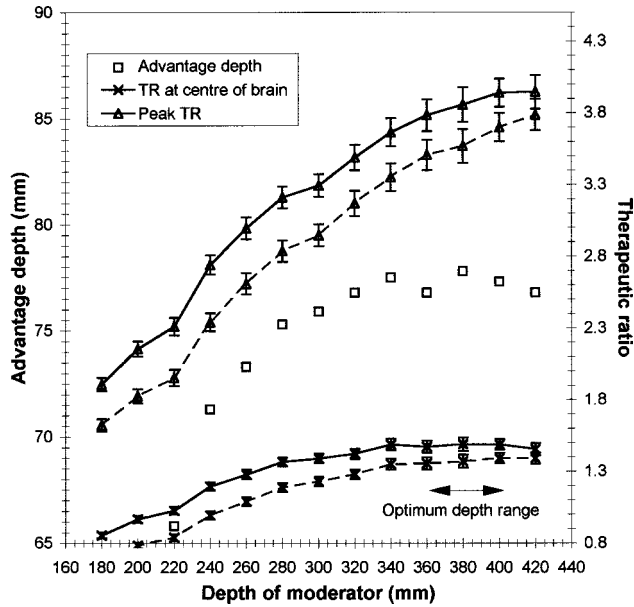


FIG. 9. The peak value of TR and TR at the center of the brain for various moderator sizes and a neutron source from 3.5 MeV protons. The range of optimum moderator size is indicated. Neutron RBE=3.2 (full lines) and 4.5 (dashed lines). The advantage depth for neutron RBE=3.2 is also plotted.

the changes would not be major. We must also remember that the actual beam neutron RBE will be dependent on the moderator size and must be determined for each proposed treatment facility.

Table II summarizes the figures of merit and treatment times for the optimum moderator sizes assuming a neutron RBE of 3.2. What is clear from this summary is that the beam quality is remarkably independent of the choice of proton energy between 2.15 and 2.8 MeV if the optimum moderator is used. For the selected proton energies up to 2.8 MeV, the TR at the center of the brain shows only a 2.4%

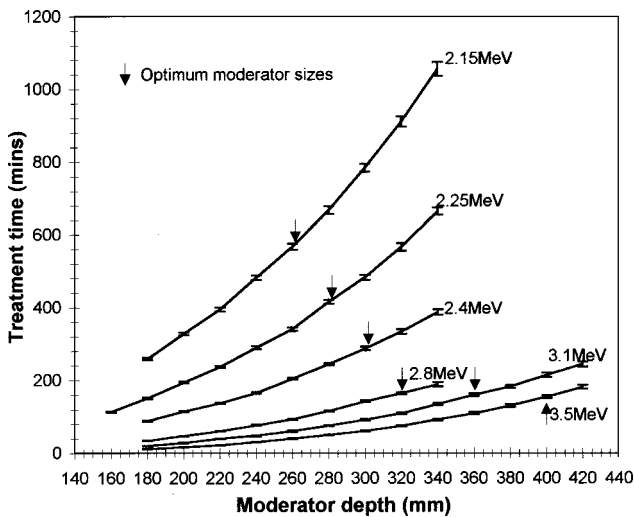


FIG. 10. Required treatment times for each moderator and proton energy configuration, assuming a 1 mA proton beam current and a maximum biologically weighted dose to healthy tissue of 12.6 Gy-Eq.

TABLE II. Summary of the in-phantom treatment planning figures of merit for the proton energies considered at the optimum moderator depth.

Proton energy (MeV)	Optimum moderator depth (mm)	Therapeutic ratio at 65 (mm)	Maximum therapeutic ratio	Advantage depth (mm)	Treatment time @ 1 mA (minutes)
2.15	260	1.70 ± 0.03	4.01 ± 0.07	81.8	567 ± 9
2.25	280	1.68 ± 0.03	4.12 ± 0.06	81.7	416 ± 6
2.4	300	1.65 ± 0.03	4.05 ± 0.08	80.9	287 ± 6
2.8	320	1.66 ± 0.03	4.10 ± 0.08	80.0	164 ± 4
3.1	360	1.58 ± 0.04	4.00 ± 0.10	79.2	160 ± 4
3.5	400	1.48 ± 0.04	3.94 ± 0.10	77.3	155 ± 4

variation, which is within the errors, the peak TR shows only a 2.4% variation, also within the errors, and the AD varies by only 2.3%. In contrast, increasing the proton energy to 3.5 MeV results in optimum figures of merit which are markedly worse than those achieved at lower projectile energies.

The treatment times required, however, are not independent of the selected proton energy. The marks on Fig. 10 for the optimum moderator sizes show that we have a steady decrease in treatment time as the incident proton energy is increased, up to 2.8 MeV. Because of the considerably larger moderator required, we see little further reduction in treatment time if a 3.5 MeV proton beam is used.

The proton energy for each of the optimum moderators is plotted against the resulting treatment time in Fig. 11. This figure shows a series of iso-current curves which demonstrate the energy and current requirements necessary to achieve a given total treatment time. All of the points on these curves below about 3.0 MeV produce, with an optimum AlF₃/Al/LiF moderator, approximately the same treatment beam quality, in terms of advantage depth, maximum therapeutic ratio and therapeutic ratio at the center of the brain. It can be seen from this figure that for a treatment time of 50 min we require 3.3 mA of 2.8 MeV protons (9.2 kW beam power). There is little advantage in using higher energies unless treatment beam quality is to be compromised.

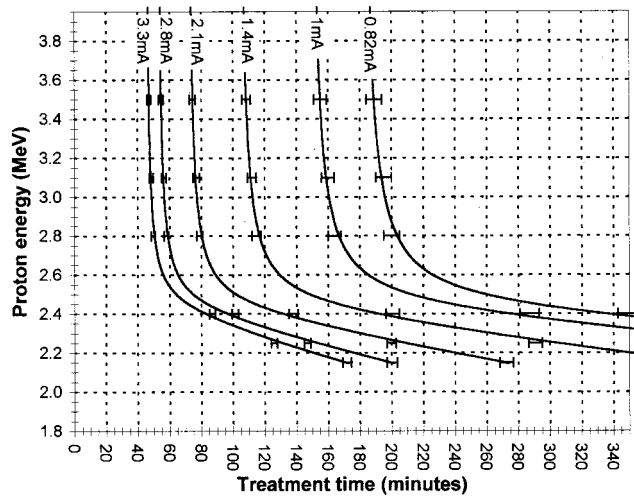


FIG. 11. Iso-current plots of proton energy against treatment time (to deliver 12.6 Gy-Eq maximum biologically weighted dose to healthy tissue) for optimized moderators.

However, if clinical requirements determine that the treatment is to be delivered in, say, four fractions of no more than 50 min each, then treatment can be achieved using the following combinations: (i) a beam current of only 0.82 mA with 2.8 MeV protons (2.3 kW beam power), (ii) a beam current of 1.4 mA with 2.4 MeV protons (3.4 kW beam power), (iii) a beam current of 2.1 mA with 2.25 MeV protons (4.2 kW beam power) or (iv) a beam current of 2.8 mA with 2.15 MeV protons (6.0 kW beam power). The advantages of choosing the highest of these proton energies (2.8 MeV) is clear from a point of view of target engineering design.

V. CONCLUSIONS

This paper has demonstrated the importance of completely coupled moderator-phantom simulations in BNCT moderator design studies. The optimum thickness of a $\text{AlF}_3/\text{Al}/\text{LiF}$ epithermal BNCT moderator has been determined, for a range of proton energies, using only in-phantom treatment planning figures of merit, without reference to empty beam parameters or fluence rates. Assuming that the proton beam current is kept constant, there is a remarkable lack of dependence of the beam quality, as indicated by the in-phantom figures of merit, upon the initial selection of proton energy up to 2.8 MeV. Going to even higher energies, however, is detrimental to the achievable beam quality. It is in the required treatment times that differences are seen between the different proton energies, with the higher proton energies producing shorter treatment times despite needing larger moderators. This reduction, however, does not continue indefinitely.

A change to the assumed value of neutron RBE from 3.2 to 4.5 makes quantitative differences to the achievable beam quality, but only small changes to the perceived optimum moderator sizes. Green and Tattam¹⁸ present a derived neutron RBE figure of 3.3 ± 0.3 for the heavy water moderated accelerator-based beam at Birmingham, based on in-phantom microdosimetric measurements. Within experimental uncertainty this value is the same as that quoted for the Brookhaven beam. However, there is an urgent need for measured RBE values for accelerator-based BNCT beams, which have very different spectra from their reactor-based counterparts.

¹D. A. Allen and T. D. Beynon, "A design study for an accelerator-based epithermal neutron beam for BNCT," *Phys. Med. Biol.* **40**, 807–821 (1995).

²J. F. Crawford and D. Suwannakachorn, "What are the best energies for neutron production for NCT?," in *Frontiers in Neutron Capture Therapy, Proceedings of the Eighth International Symposium on Neutron Capture Therapy for Cancer*, edited by M. F. Hawthorne *et al.* (Plenum, New York) (in press).

³R. J. Kudchadker, J. F. Kunze, and J. F. Harmon, "Balancing neutron yield and moderator dimensions in accelerator sources," in *Advances in Neutron Capture Therapy*, Excerpta Medica, International Congress Series 1132, edited by B. Larsson, J. Crawford, and R. Weinreich, (Elsevier, Amsterdam, 1997), Vol. I, pp. 516–521.

⁴S. Zimin and B. J. Allen, "Study of moderator thickness for an accelerator-based neutron irradiation facility for boron neutron capture therapy using the ${}^7\text{Li}(p,n)$ reaction near threshold," *Phys. Med. Biol.* **45**, 59–67 (2000).

⁵D. L. Bleuel, R. J. Donahue, B. A. Ludewigt, and J. Vujic, "Designing accelerator-based epithermal neutron beams for boron neutron capture therapy," *Med. Phys.* **25**, 1725–1734 (1998).

⁶V. N. Kononov, V. I. Regushevskiy, N. A. Soloviev, and A. I. Leipunskiy, "Accelerator-based intense and directed neutron source for BNCT," in *Advances in Neutron Capture Therapy*, Excerpta Medica, International Congress Series 1132, edited by B. Larsson, J. Crawford, R. Weinreich (Elsevier, Amsterdam, 1997), Vol. I, pp. 528–532.

⁷H. Liskien and A. Paulsen, "Neutron production cross-sections and energies for the reactions ${}^7\text{Li}(p,n){}^7\text{Be}$ and ${}^7\text{Li}(p,n){}^7\text{Be}^*$ (431 keV)," *At. Data Nucl. Data Tables* **15**, 57–84 (1975).

⁸J. Campbell and M. C. Scott, "Absolute neutron yield measurements for protons on Li, Cu, Co and Be from threshold to 3 MeV," in *Scientific and Industrial Applications of Small Accelerators*, 4th Conference, Denton, TX, 1976 (IEEE, New York, 1976).

⁹J. F. Briesmeister, "MCNP—A general purpose n -particle transport code version 4B," LA-12625-M, Los Alamos National Lab., 1997.

¹⁰D. A. Allen, T. D. Beynon, and S. Green, "Design for an accelerator-based orthogonal epithermal neutron beam for boron neutron capture therapy," *Med. Phys.* **25**, 71–76 (1999).

¹¹B. V. Harrington, "Optimization of an epithermal beam in HIFAR for boron neutron capture therapy," ANSTO/E662, Lucas Heights Research Lab., New South Wales, Australia, 1987.

¹²W. S. Snyder, M. R. Ford, G. G. Warner, and H. L. Fisher, Jr., "Estimates of absorbed fractions for monoenergetic photon sources uniformly distributed in various organs of a heterogeneous phantom (Appendix B)," *J. Nucl. Med., MIRD Supplement No. 3*, Pamphlet 5 (1969).

¹³H. B. Liu, D. D. Greenberg, J. Cappala, and F. Wheeler, "An improved neutron collimator for brain tumour irradiations in clinical boron neutron capture therapy," *Med. Phys.* **23**, 2051–2060 (1996).

¹⁴J. A. Coderre, M. S. Makar, P. L. Micca, M. M. Nawrocky, H. B. Liu, D. D. Joel, D. N. Slatkin, and H. I. Amols, "Derivations of relative biological effectiveness for the high LET radiations produced during boron neutron capture irradiations of the 9L rat gliosarcoma in vitro and in vivo," *Int. J. Radiat. Oncol., Biol., Phys.* **27**, 1121–1129 (1993).

¹⁵G. M. Morris, J. A. Coderre, J. W. Hopewell, P. L. Micca, M. M. Nawrocky, H. B. Liu, and A. Bywaters, "Response of the central nervous system to boron neutron capture irradiation: Evaluation using rat spinal cord model," *Radiother. Oncol.* **32**, 249–255 (1994).

¹⁶S. A. Wallace, J. N. Mathur, and B. J. Allen, "Treatment planning figures of merit in thermal and epithermal boron neutron capture therapy of brain tumours," *Phys. Med. Biol.* **39**, 897–906 (1994).

¹⁷J. Capala, M. Chadha, J. A. Coderre, A. Z. Diaz, H. B. Liu, F. J. Wheeler, D. E. Wessol, L. Wielopolski, and A. D. Chanana, "Radiation doses to brain under the BNCT protocols at Brookhaven National Laboratory," in *Advances in Neutron Capture Therapy*, edited by B. Larsson, J. Crawford, and R. Weinreich, Excerpta Medica, International Congress Series 1132 (Elsevier, Amsterdam, 1997), pp. 51–55.

¹⁸S. Green and D. Tattam, "Determination of the RBE of an epithermal neutron beam for BNCT from microdosimetric measurements," in *Frontiers in Neutron Capture Therapy, Proceedings of the Eighth International Symposium on Neutron Capture Therapy for Cancer*, edited by M. F. Hawthorne *et al.* (in press).